8-22-2016

The Construction of Acoustic Waveforms from Plane Wave Components to Enhance Energy Transmission into Solid Media

Daniel C. Woods
Purdue University, woods41@purdue.edu

J Stuart Bolton
Purdue University, bolton@purdue.edu

Jeffrey F. Rhoads
Purdue University, jfrhoads@purdue.edu

The Construction of Acoustic Waveforms from Plane Wave Components to Enhance Energy Transmission into Solid Media

Daniel C. Woods, J. Stuart Bolton, and Jeffrey F. Rhoads

School of Mechanical Engineering,
Ray W. Herrick Laboratories,
and Birck Nanotechnology Center,
Purdue University
West Lafayette, Indiana, USA

August 22, 2016

Introduction

- Goal is to tune the spatial wave profile to maximize the transmitted energy across fluid-solid interfaces

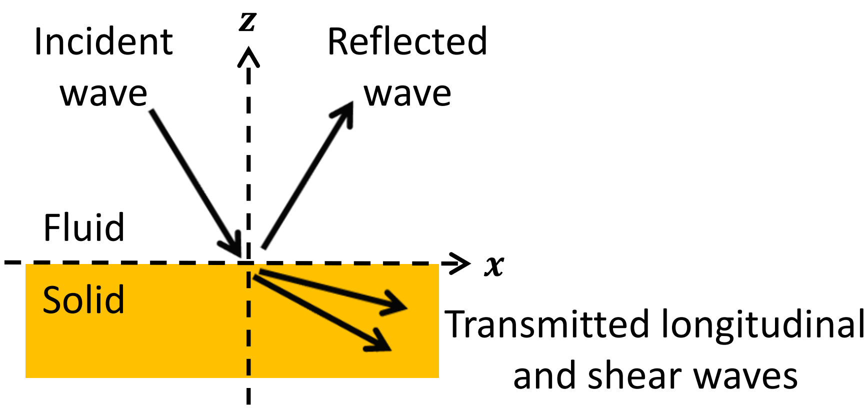

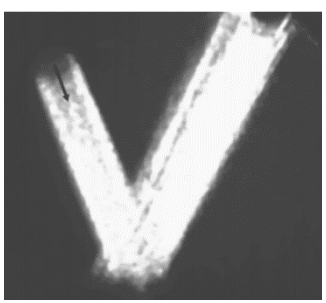

Teklu et al., J. Appl. Phys., 2005.

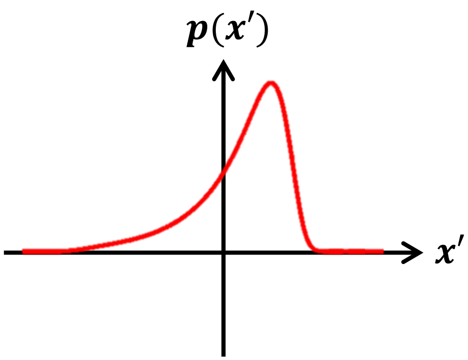

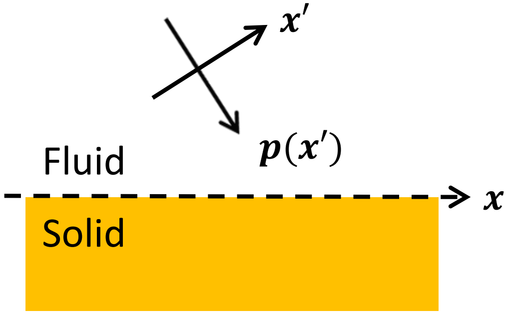

Introduction

- Potential applications for enhanced acoustic energy transmission into solid materials:
  - Nondestructive structural testing
  - Medical ultrasound imaging and ablation
  - Other, non-contact ultrasound applications

(*Image credit: http://ndtoverseas.org/Conventional%20Non%20Destructive%20Test.html*)

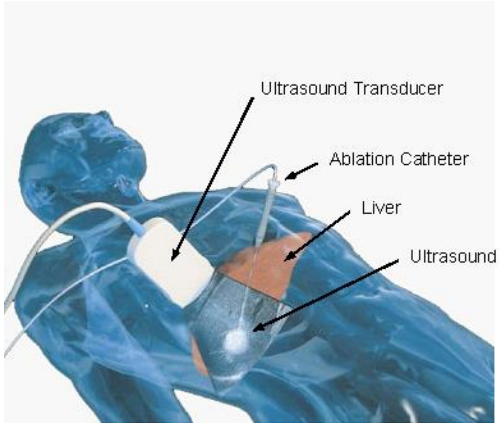

(*Image credit: http://academicdepartments.musc.edu/sebin/x/k/tumor_abl_overview.jpg*)

Results for Plane Waves

- Minimum in reflection can be achieved by varying spatial decay rate β near the Rayleigh angle

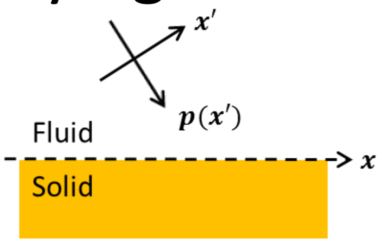

Exemplary Fluid—Solid Interface: Magnitude of Reflection Coefficient

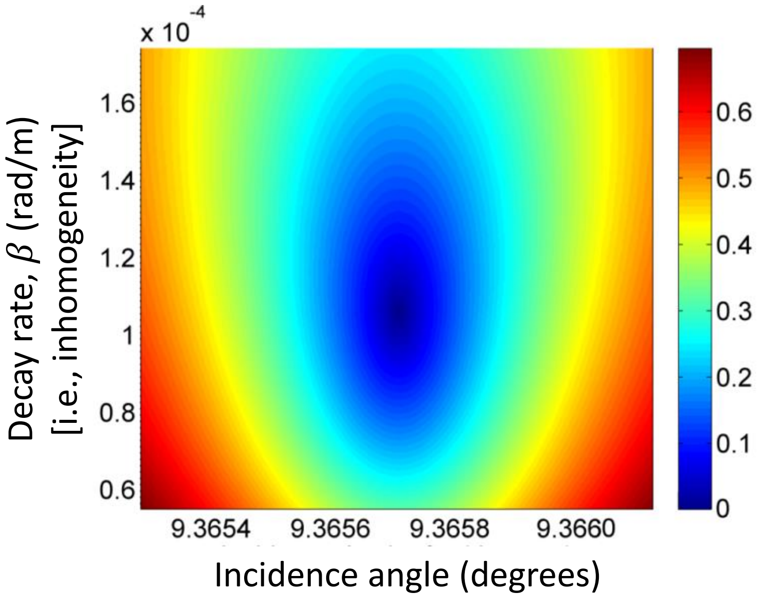

(*adapted from Woods et al., J. Acoustical Soc. Am.*, 2015)

Homogeneous plane wave

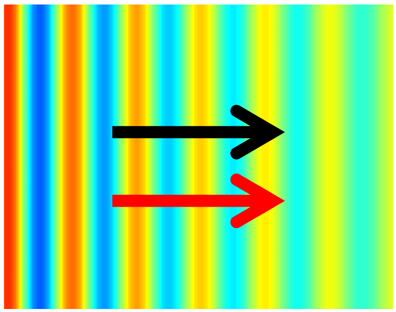

Inhomogeneous plane wave

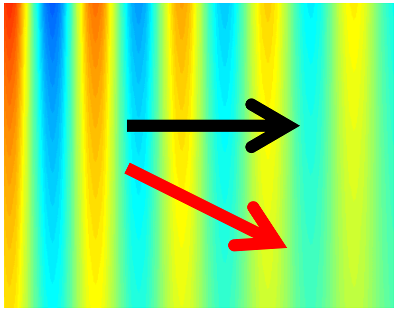

Additional component of amplitude decay, $\exp(-\beta\delta)$

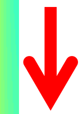

Results for Plane Waves

- Minimum in reflection can be achieved by varying spatial decay rate β near the Rayleigh angle

Exemplary Fluid—Solid Interface: Magnitude of Reflection Coefficient

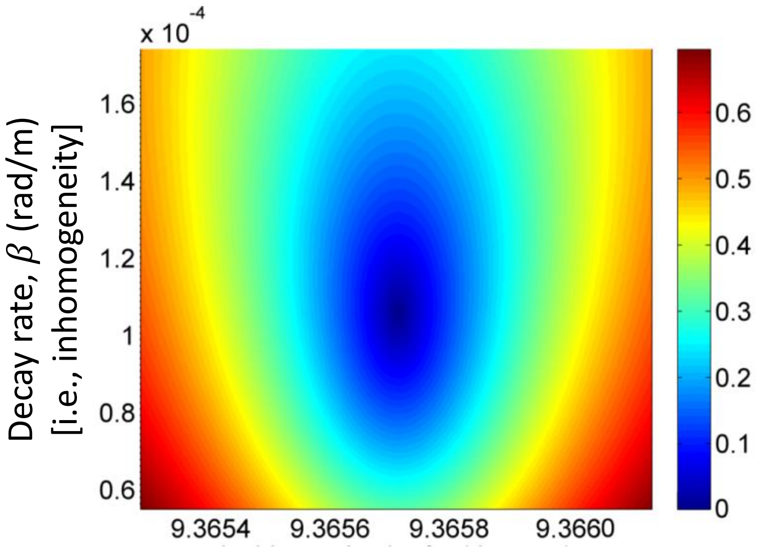

(*adapted from Woods et al., J. Acoustical Soc. Am.*, 2015)

Reduction of Reflection Coefficient Near Rayleigh Angle

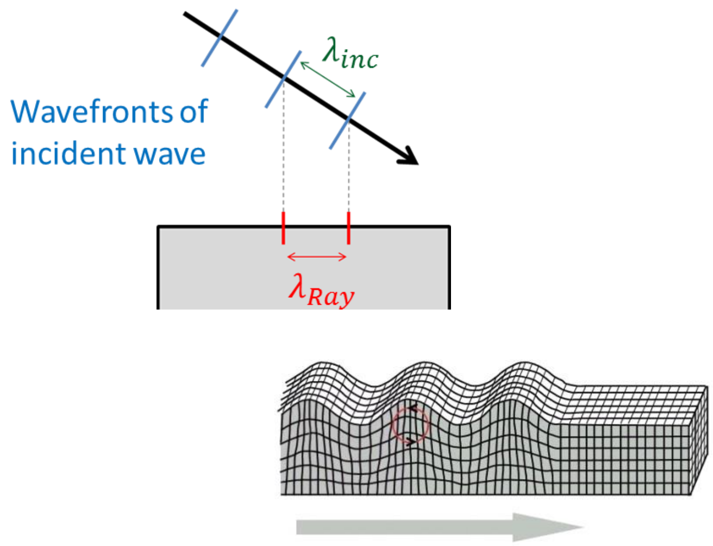

Spatial resonance of induced longitudinal and shear particle motions

(*Image credit: http://www.sjvgeology.org/oil/Rayleigh_surface_waves2.gif*)

Bounded Wave Profiles

- Versatile form to model the incident wave pressure profile:

$$\tilde{p}(x',0) = \tilde{A}\exp\left[\beta x' - \frac{1}{\alpha}\left(\frac{|x'|}{W}\right)^{\alpha}\right]\exp(-j\omega t)$$

(form adapted from Vanaverbeke et al., J. Acoustical Soc. Am., 2003)

$\alpha = 2$: Gaussian wave
$\alpha = 8$: "Square" wave

(i.e., when $\beta = 0$)

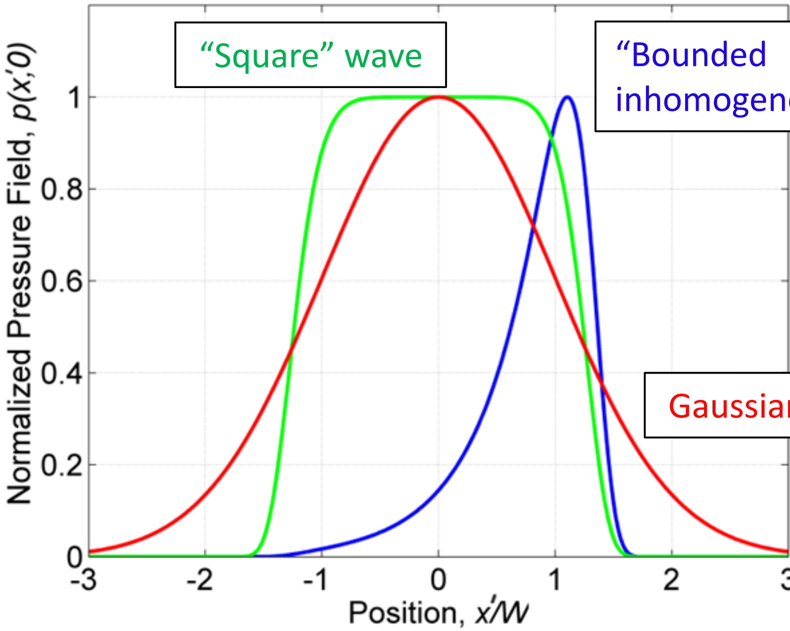

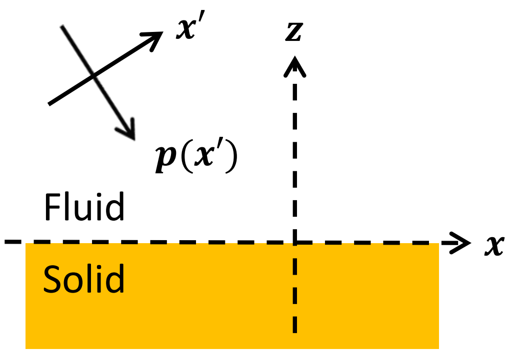

Bounded Wave Profiles

- Analysis requires Fourier decomposition into plane wave components

Incident wave parameters → **Wavenumber decomposition** → **Reflection and transmission coefficients** → **Transmitted stresses, particle motions, energy**

Incident wave parameters: Spatial form of pressure, as well as amplitude and frequency

Wavenumber decomposition: Fourier transform of incident wave profile into plane wave components

Reflection and transmission coefficients: Apply plane wave theory for each plane wave component

Transmitted stresses, particle motions, energy: Summation of the contributions from the transmitted longitudinal and shear wave components

↓ (from Incident wave parameters)

Can vary parameters to maximize, e.g., surface wave excitation, transmitted stresses, etc.

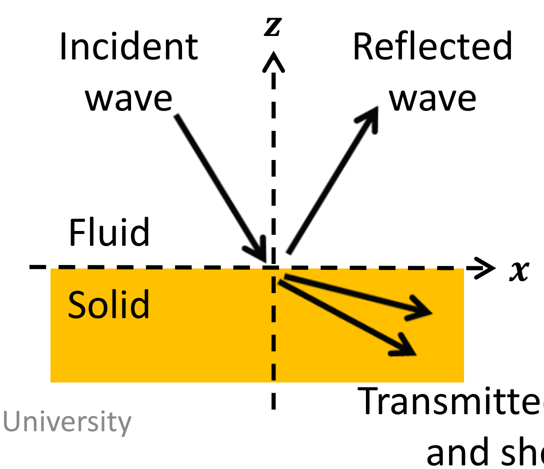

Surface Wave Excitation Efficiency

- Measure of the penetration of the incident wave energy and subsequent excitation of the solid surface wave

$$\eta(x) = \frac{\int_{-\infty}^{x} \left[\left| I_{inc,z}(\xi,0) \right| - \left| I_{R,z}(\xi,0) \right| \right] d\xi}{\int_{-\infty}^{+\infty} \left| I_{inc,z}(\xi,0) \right| d\xi}$$

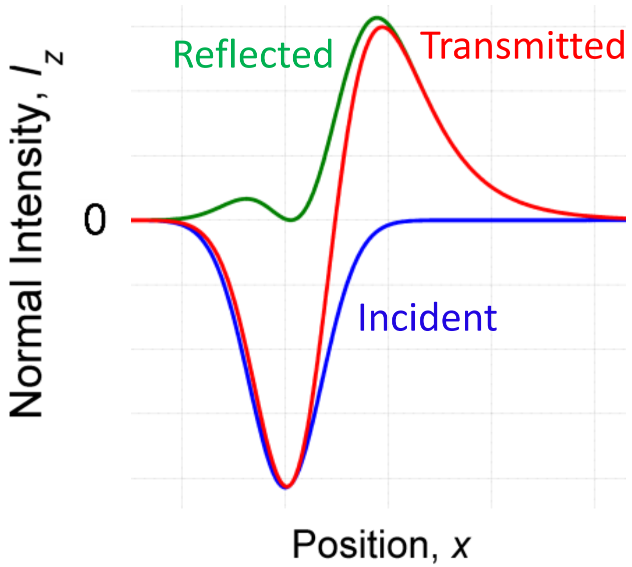

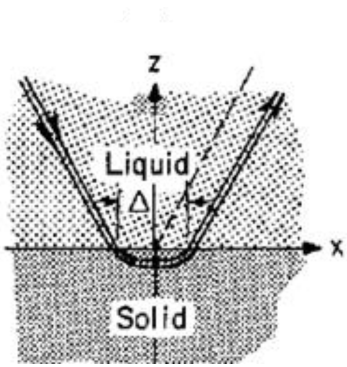

Bertoni & Tamir, Appl. Phys., 1973.

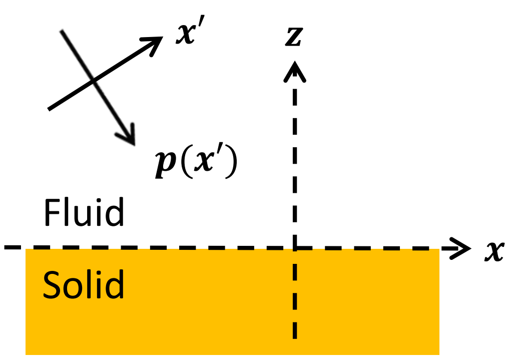

Results for Water—Stainless Steel Interface

Surface Wave Excitation Efficiency, $\eta(x^*)$

Square/Gaussian Incident Waves

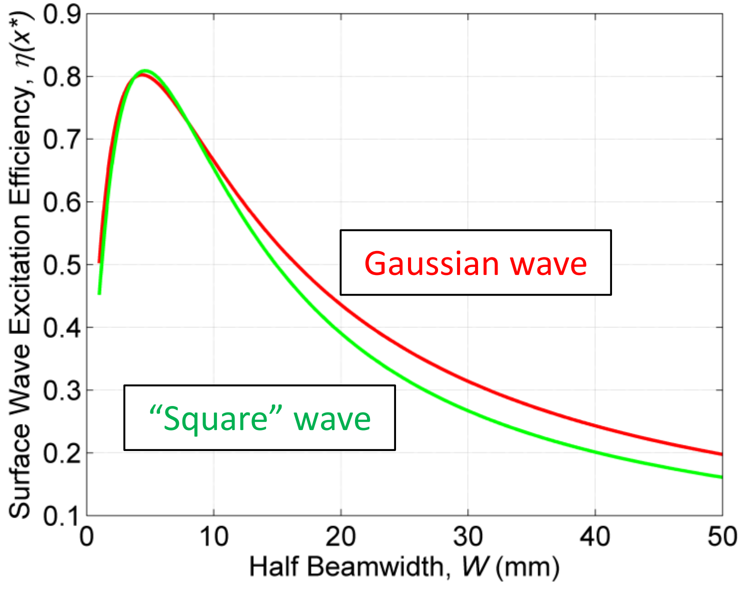

"Bounded Inhomogeneous" Incident Waves

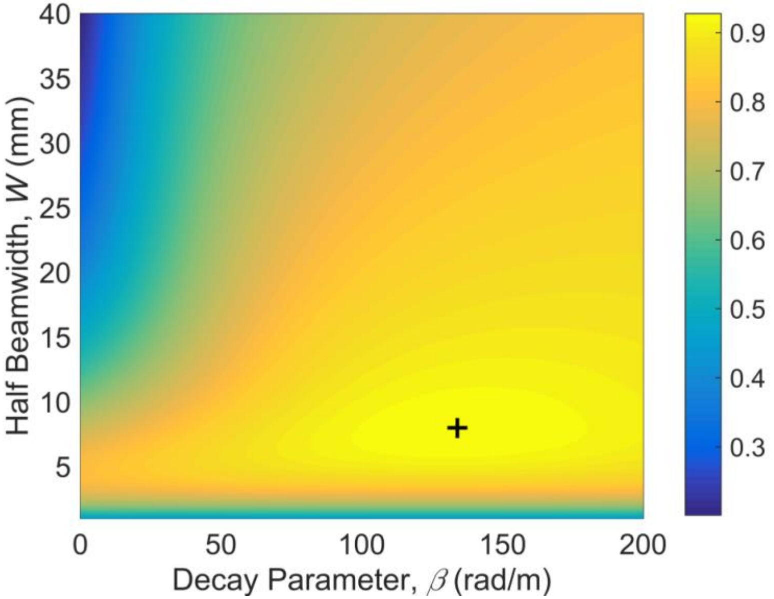

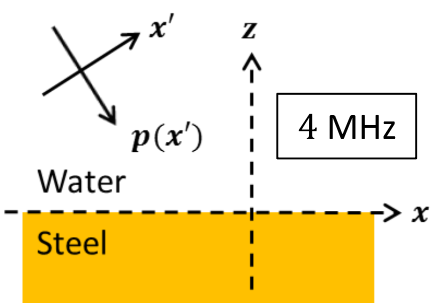

Results for Water—Stainless Steel Interface

Induced Stresses in Stainless Steel, $|\tilde{\sigma}_{zz}|$ (MPa)

Square wave
($\beta = 0, W = 7.7$ mm)

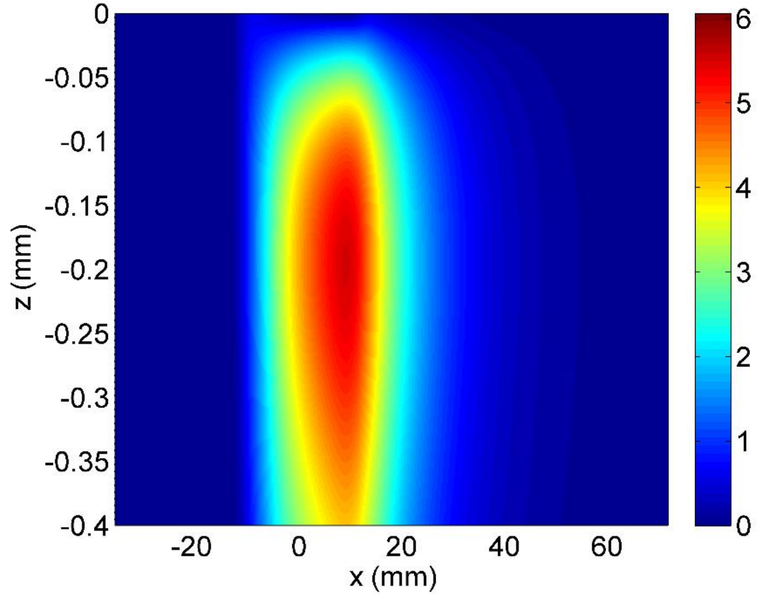

Bounded inhomogeneous wave
($\beta = 134.2$ m^{-1}$, W = 7.7$ mm)

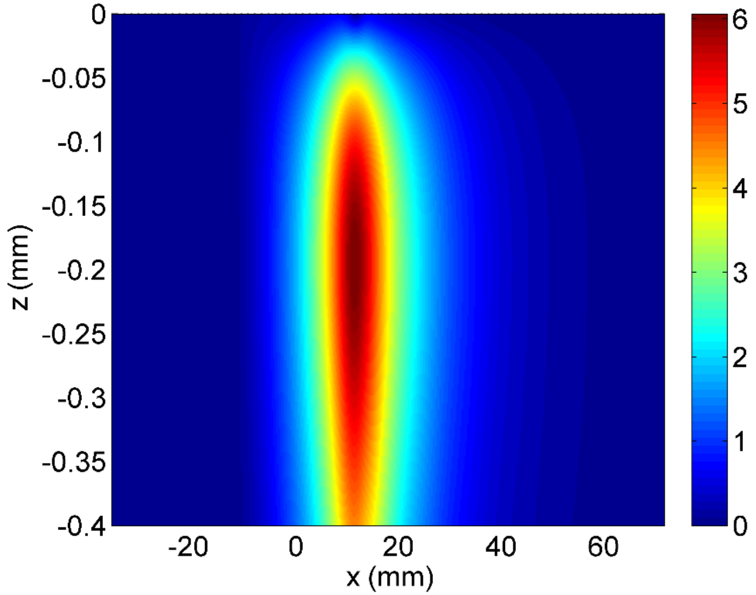

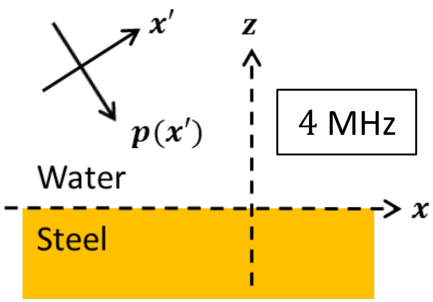

Results for Water—Stainless Steel Interface

Induced Particle Velocities, $|\tilde{v}_z|$ (m/s)

Square wave
($\beta = 0, W = 7.7$ mm)

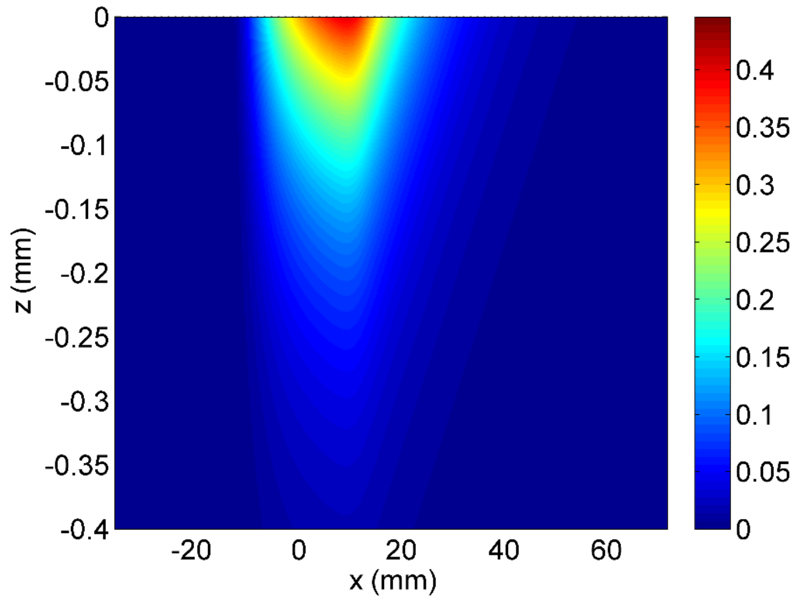

Bounded inhomogeneous wave
($\beta = 134.2$ m^{-1}$, W = 7.7$ mm)

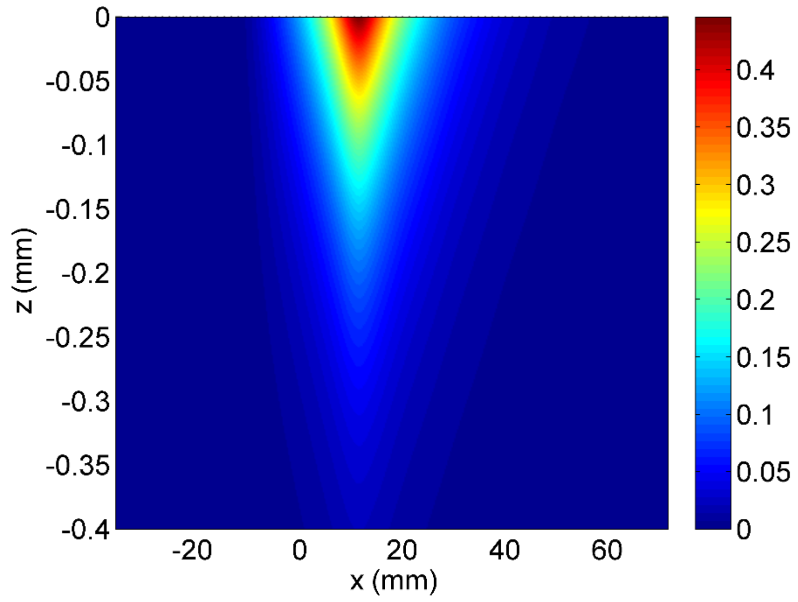

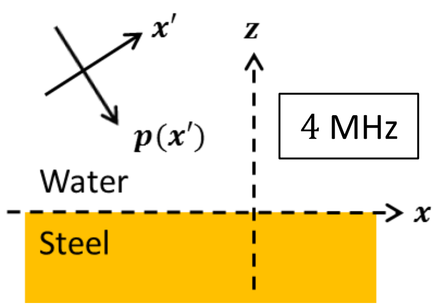

Results for Water—Stainless Steel Interface

Induced Normal Intensities, $|I_z|$ (W/mm²)

Square wave
($\beta = 0, W = 7.7$ mm)

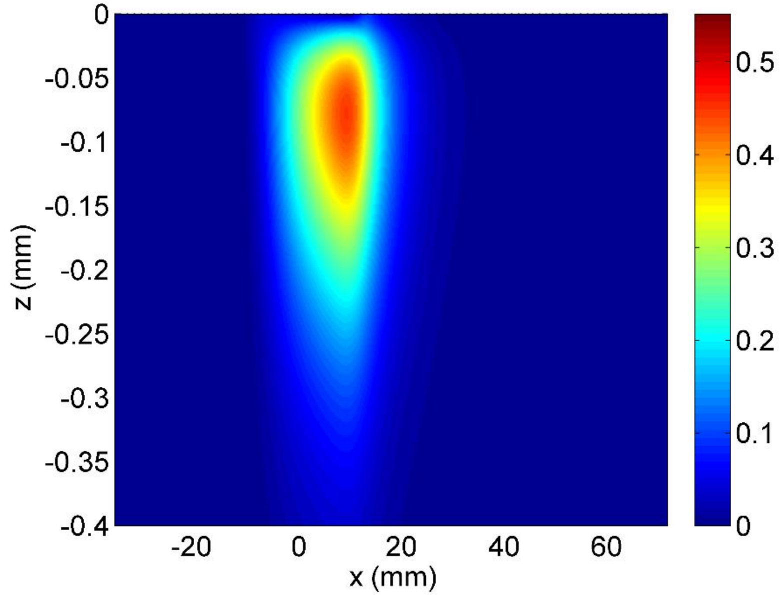

Bounded inhomogeneous wave
($\beta = 134.2$ m^{-1}$, W = 7.7$ mm)

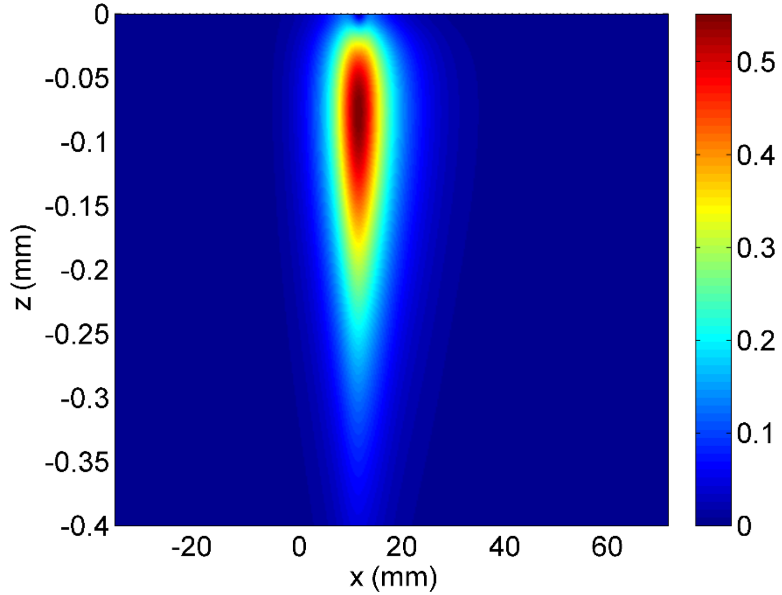

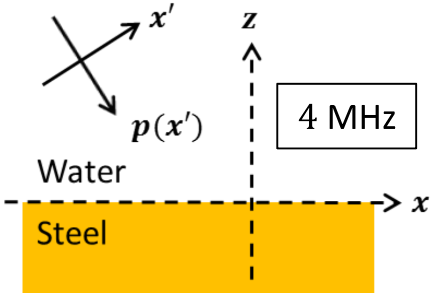

Effect of Material Dissipation

Surface Wave Excitation Efficiency, $\eta(x^*)$

Lossless Solid

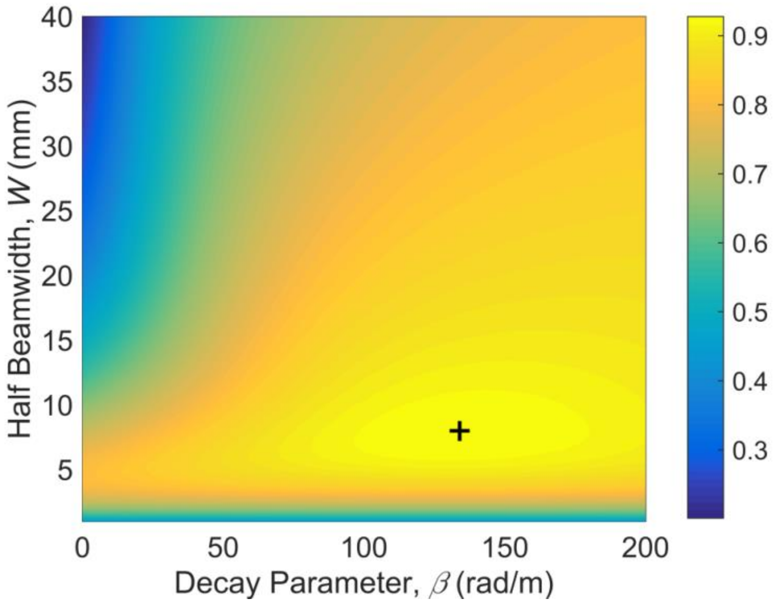

Viscoelastic Solid

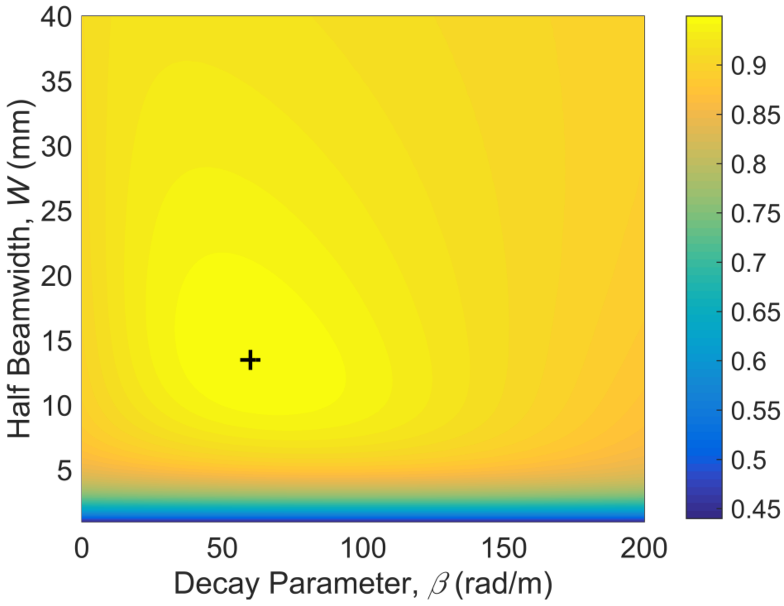

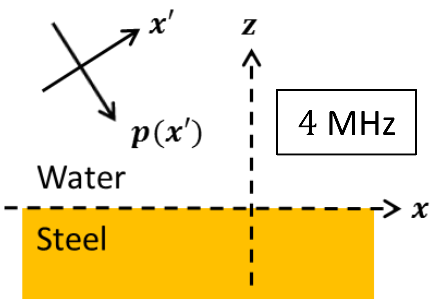

Results with Material Dissipation

Induced Stresses in Stainless Steel, $|\tilde{\sigma}_{zz}|$ (MPa)

Square wave
($\beta = 0, W = 13.5$ mm)

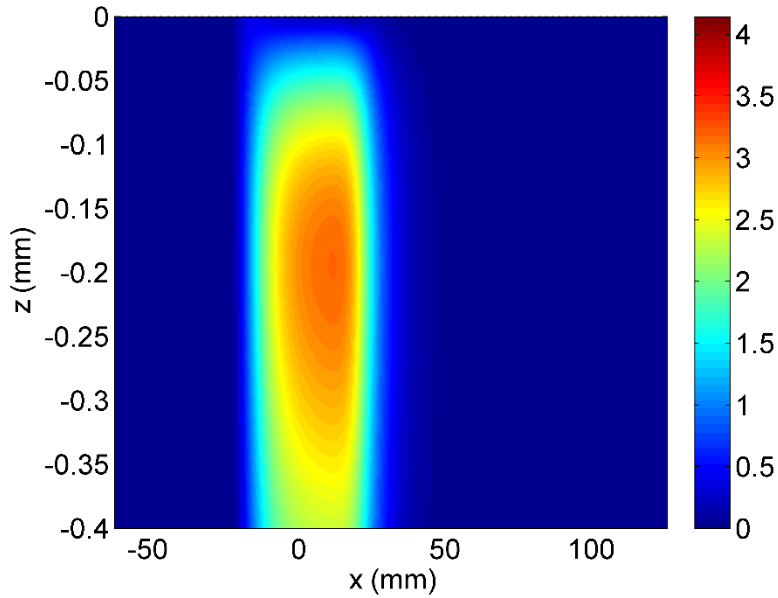

Bounded inhomogeneous wave
($\beta = 59.8$ m^{-1}$, W = 13.5$ mm)

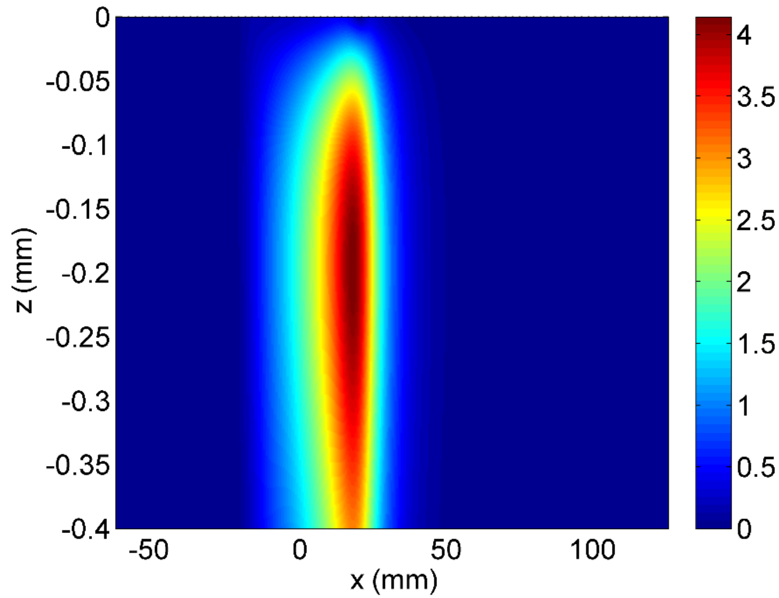

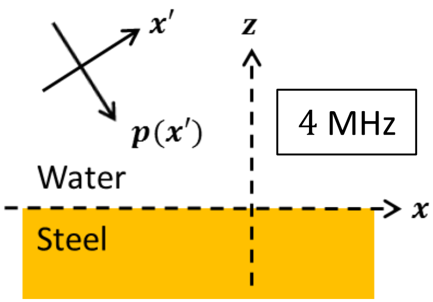

Results with Material Dissipation

Induced Normal Intensities, $|I_z|$ (W/mm²)

Square wave
($\beta = 0, W = 13.5$ mm)

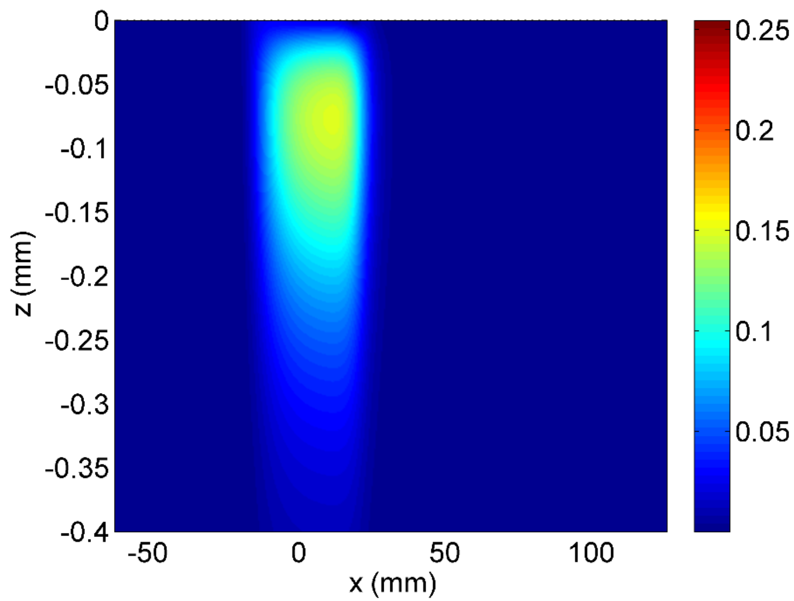

Bounded inhomogeneous wave
($\beta = 59.8$ m⁻¹$, W = 13.5$ mm)

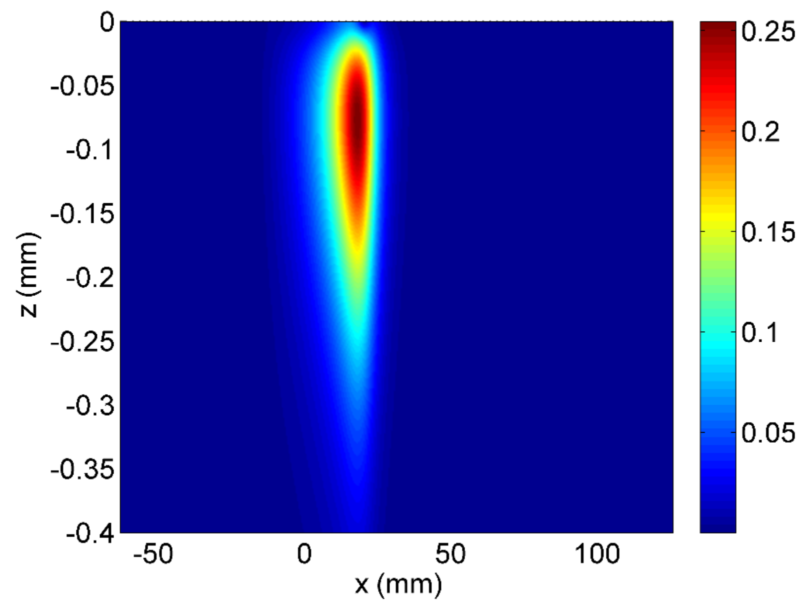

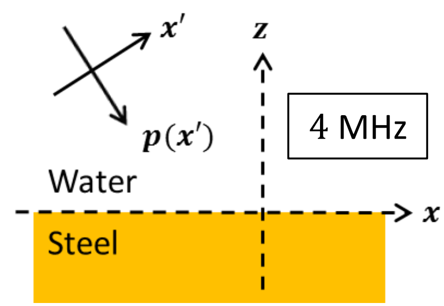

Conclusions

- Investigation of tunable "bounded inhomogeneous" incident wave profiles for enhanced transmission across fluid—solid interfaces
  - Increased surface wave excitation efficiency
  - Increased subsurface stress and energy flux
- Material dissipation causes a shift in the optimal profile parameters (lower degree of asymmetry, larger beamwidth)

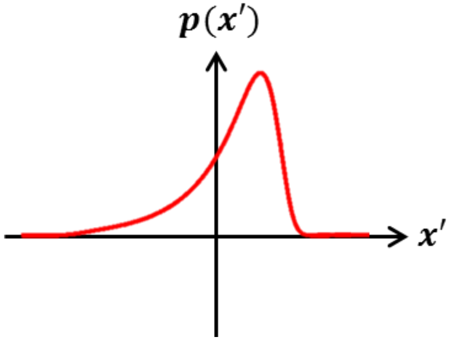

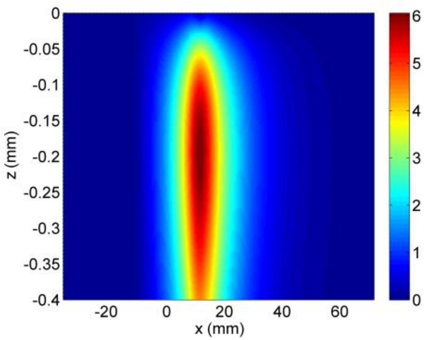

Next Steps in Investigation of Waveforms

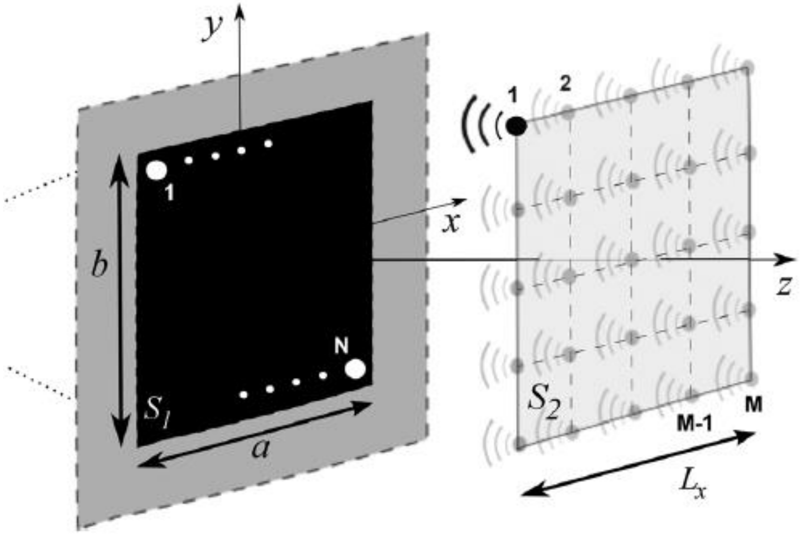

Generation of these types of profiles by phased arrays
(image adapted from Robin et al., J. Acoustical Soc. Am., 2014)

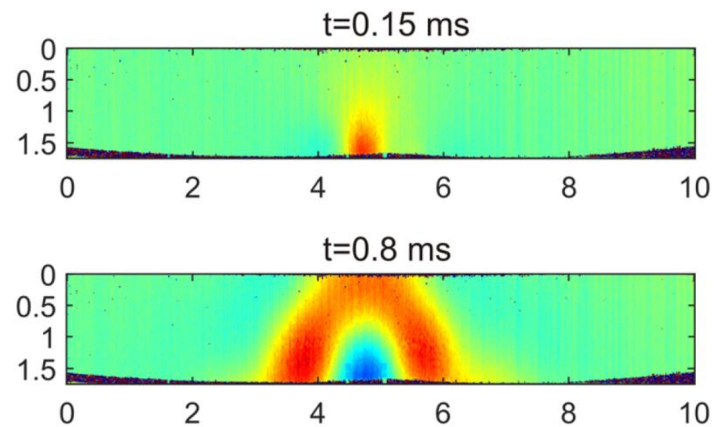

Analysis of pulse excitation by various waveforms
(image adapted from Ambrozinski et al., Appl. Phys. Lett., 2016)

Acknowledgement

The authors would like to thank the U.S. Office of Naval Research for its support of this research under ONR Grant No. N00014-10-1-0958.